YU ISSN 0015—3206
FZKAAA 14 (2) 77 (1982)

THEORY OF THE ELECTRON-SURFACE-POLARITON INTERACTION. APPLICATION TO ELECTRON-TRANSMISSION EXPERIMENTS

M. S. TOMAŠ

Ruder Bošković Institute, Zagreb, Croatia, Yugoslavia

Z. LENAC*

Pedagogical Faculty, Rijeka, Yugoslavia

M. ŠUNJIĆ

Department of Physics, Faculty of Science, P. O. B. 162, Zagreb, Croatia, Yugoslavia

Received 24 October 1981

UDC 538.97

Original scientific paper

The interaction of a non-relativistic charged particle with a surface polariton in a crystal slab is formulated quantum mechanically and applied to calculate probabilities of surface-polariton emission. The electron energy-loss function relevant for electron-transmission experiments is calculated in the Born approximation. Retardation corrections to the electron spectrum are discussed for a dielectric and a metallic slab at normal electron incidence and for single- and multiple-scattering processes.

1. Introduction

Quantum-mechanical formulations of the problem of interaction of charges with long-wavelength collective excitations in thin crystal foils have been considered in connection with various problems, such as electron tunnelling[1], low-

*Also at the Rudjer Bošković Institute, Zagreb, Croatia, Yugoslavia.

-energy-electron diffraction and photoemission[2], electron transmission[3,4], etc. Extensive reviews of this subject can be found in Ref. 5. However, as a rule, the retardation of the electromagnetic field, which becomes important in the extreme long-wavelength limit, was neglected in these approaches. Instead of dealing with surface polaritons (coupled photon-surface phonon or plasmon excitations), the theories treated their quasi-static counterparts (surface phonons or plasmons). Although this approximation is often physically valid, there are cases when the retardation of the electromagnetic field must be taken into account, e. g. in interpreting the experimental data obtained in electron-transmission spectroscopy[6].

Inelastic processes in which electrons transmitted through a thin foil lose their energy in exciting surface collective oscillations were first studied classically[7-9] in a quasi-static approximation. These theories described the observed electron spectra satisfactorily and assumed that the retardation of the electromagnetic field had little influence in such experiments. However, in measuring electron energy losses on Al, Schmüser[10] and Boersch et al.[11] obtained apparently different results for the dependence of surface-mode maxima on foil thickness. This contradiction was removed by observing that in interpreting the spectra, one should use a theory which takes into account the retardation of the electromagnetic field[12], as was later verified experimentally[12-14]. Since retardation changes the surface-mode dispersion drastically in the extreme long-wavelength region, it became clear that the main difficulty in observing its effects on the energy-loss spectra lies in the low angular sensitivity of the experimental apparatus. However, some years ago measurements were performed [15-19] with an angular resolution of approximately 8×10^{-6} rad, almost an order of magnitude better than in previous experiments. These measurements show that, in view of accuracy, the electron-transmission spectroscopy of surface excitations may become comparable with existing optical experiments and complementary to them because of a very large energy region it covers.

The aim of this work is primarily to construct a quantum theory of the surface-polariton — electron interaction, i. e. to extend the quantized-Hamiltonian formalism to the slab geometry, and thus provide the basis for further theoretical investigations of surface-polariton properties and various effects associated with their interaction with charged particles.

We apply our theory to the calculation of electron energy-loss spectra in transmission experiments, our considerations being motivated by the experiments[15-19] which, owing to the special techniques used, allow the investigation of the extreme long-wavelength region where retardation effects are most important. Although the classical dielectric theory[20-22] leads to proper results (for first-order processes), we feel that the quantum-mechanical approach should better explain retardation effects in such experiments for two reasons:

(i) The true dispersion relations of surface modes appear from the beginning, and not as poles in the energy-loss function. Therefore, the contribution of each surface mode can be calculated and discussed separately.

(ii) The quantum-mechanical approach allows the calculation of higher-order processes, i. e. multiple-excitation probabilities, which have so far been calculated only in the quasi-static approximation[3,4].

On the other hand, the damping of surface modes, which is included in the classical theory immediately by using the complex dielectric function, should, in

our approach, be calculated separately (using the method of Nkoma et al.[23], for example). In this paper, therefore, we study the main features of the theoretical surface-electron energy-loss spectrum, namely the influence of retardation on the strength and positions of loss peaks, neglecting in the first approximation the damping of surface modes[24] and also the effects associated with the presence of an overlayer[25].

In Sect. 2 we quantize the long-wavelength surface-polariton field starting from the point-ion model of the dielectric slab and following the method of quantization already used for a semi-infinite crystal[26]. Then we generalize the results to describe a more general situation, e. g. a surface-polariton field in any crystal slab with a real dielectric function.

In Sect. 3 we include the interaction of surface polaritons with an electron and calculate the probability of surface-polariton emission in the Born approximation. For the electron energy much higher than the energy of polaritons, as is always the case in transmission experiments, the electron recoil during the scattering may be neglected (the so-called fast-electron approximation[3,4]). In this approximation, our quantum-mechanical result leads to an electron energy-loss function which coincides, for a real dielectric function, with the classical result. In addition, the neglect of electron recoil opens the possibility of turning the theory into the semiclassical one, the electron representing just the classical current. In this way, one can easily calculate processes of all orders using standard methods, as performed, for example, in Refs. 3 and 4. We explore this possibility in Sect. 4.

In Sect. 4 we discuss surface losses for electrons transmitted through a slab and analyze the effects of retardation on the electron spectra in a dielectric and a metallic slab. We make a comparison with the previously obtained results and with experiments. We also suggest some further possible investigations.

2. *The free-surface-polariton Hamiltonian*

We quantize the surface-polariton field in a thin film, closely following the method of Ref. 26, where it was applied to a semi-infinite solid.

We start with the point-ion model of a dielectric slab in vacuum, occupying the region $|z| \leq a$ and extending infinitely in the x and y directions. We look for a solution of the polarization vector in the form $\vec{P}(\vec{r}, t) \sim \vec{P}_{\vec{k}}(z) \exp(\mathrm{i}\vec{k} \cdot \vec{\varrho} - \mathrm{i}\omega t)$ (where $\varrho = (x, y)$ and $\vec{k} = (k_x, k_y)$). The wave vector $\vec{k}$ is made discrete by limiting the considerations to the surface of area A and adopting periodic boundary conditions. Now, we write Maxwell equations with $-\nabla \vec{P}$ and $\partial \vec{P}/\partial t$ as the charge and current density, respectively. Together with the equation of motion for the polarization vector and the usual boundary conditions, the Maxwell equations determine the normal modes of the system. As Kliewer and Fuchs[27] have shown, there exist two surface modes with frequencies $\omega_{\pm}(k)$ satisfying the dispersion relation

$$\varepsilon(\omega_{\pm}) = -a/a_0 \, (\mathrm{th}\, aa)^{\pm 1}, \tag{1}$$

where α and α_0 are real quantities defined by

$$\alpha = \left(k^2 - \varepsilon \frac{\omega^2}{c^2}\right)^{1/2}, \qquad \alpha_0 = \left(k^2 - \frac{\omega^2}{c^2}\right)^{1/2} \tag{2}$$

and $\varepsilon(\omega)$ is the long-wavelength dielectric function of the slab. In the point-ion model considered here,

$$\varepsilon(\omega) = 1 + \frac{\omega_P^2}{\omega_T^2 - \omega^2}, \tag{3}$$

ω_T and ω_P being *TO* and ion-plasma frequencies of the dielectric, respectively.

The corresponding polarization eigenvectors have the form

$$\begin{aligned} \vec{P}_{\vec{k}+}(z) &= C_{\vec{k}+}(\mathrm{i}\hat{k}\,\mathrm{sh}\,\alpha z + \hat{z}\,\frac{k}{\alpha}\,\mathrm{ch}\,\alpha z), \\ \vec{P}_{\vec{k}-}(z) &= C_{\vec{k}-}(\mathrm{i}\hat{k}\,\mathrm{ch}\,\alpha z + \hat{z}\,\frac{k}{\alpha}\,\mathrm{sh}\,\alpha z), \end{aligned} \tag{4}$$

where $\hat{k}$ and $\hat{z}$ are unit vectors in the $\vec{k}$ and $\vec{z}$ directions, respectively, and $C_{\vec{k}}$'s are some constants to be determined by an appropriate choice of normalization.

From the polarization eigenvectors we can easily compute the electromagnetic fields, i. e. electric- and magnetic-field eigenvectors. Introducing the usual scalar (Φ) and vector ($\vec{A}$) potentials and choosing the Coulomb gauge, we find

$$\begin{aligned} \Phi_{\vec{k}\nu}(z) &= -2\pi \int_{-a}^{a} \mathrm{d}z'\, \mathrm{e}^{-k|z-z'|}\, \vec{\chi} \cdot \vec{P}_{\vec{k}\nu}(z'), \\ \vec{A}_{\vec{k}\nu}(z) &= 2\pi \mathrm{i} \frac{c\,k}{\omega_{\vec{k}\nu}} \int_{-a}^{a} \mathrm{d}z'\, [\mathrm{e}^{-k|z-z'|}\, \vec{\chi}\,\vec{\chi} \cdot \vec{P}_{\vec{k}\nu}(z') \\ &\quad - \frac{k}{\alpha_0}\, \mathrm{e}^{-\alpha_0|z-z'|}\, \vec{\chi}'\,\vec{\chi}' \cdot P_{\vec{k}\nu}(z')], \end{aligned} \tag{5}$$

where the index ν takes two values, $\nu = +$ or $-$, and we have introduced the abbreviations

$$\vec{\chi} = \mathrm{i}\hat{k} - \hat{z}\,\mathrm{sign}\,(z - z'), \qquad \vec{\chi}' = \mathrm{i}\hat{k}\frac{\alpha_0}{k} - \hat{z}\,\mathrm{sign}\,(z - z').$$

The explicit form of $\Phi_{\vec{k}\nu}(z)$ and $\vec{A}_{\vec{k}\nu}(z)$ can be found by a straightforward integration of (5).

The quantization of the surface-polariton field can be performed as in Ref. 26. We start from the Hamiltonian:

$$H_P = \int \mathrm{d}^3 \vec{r} \left\{ \frac{1}{8\pi} \left[\frac{1}{c^2} \dot{\vec{A}}^2 + (\nabla \times \vec{A})^2 - (\nabla \Phi)^2 \right] + \right.$$
$$\left. + \frac{2\pi}{\omega_P^2} [\dot{\vec{P}}^2 + \omega_T^2 \vec{P}] + \vec{P} \nabla \Phi \right\} \tag{6}$$

and expand the fields in the following way:

$$\Phi(\vec{r}, t) = \sum_{\vec{k}n} \Phi_{\vec{k}\nu}(z) \, \mathrm{e}^{\mathrm{i}\vec{k}\vec{\varrho}} \lambda_{\vec{k}\nu} (a_{\vec{k}\nu} + a^*_{-\vec{k}\nu}),$$
$$\vec{P}(\vec{r}, t) = \sum_{\vec{k}\nu} \vec{P}_{\vec{k}\nu}(z) \, \mathrm{e}^{\mathrm{i}\vec{k}\vec{\varrho}} \lambda_{\vec{k}\nu} (a_{\vec{k}\nu} + a^*_{-\vec{k}\nu}), \tag{7}$$
$$\vec{A}(\vec{r}, t) = \Sigma_{\vec{k}\nu} \vec{A}_{\vec{k}\nu}(z) \, \mathrm{e}^{\mathrm{i}\vec{k}\vec{\varrho}} \lambda_{\vec{k}\nu} (a_{\vec{k}\nu} - a^*_{-\vec{k}\nu}).$$

The constants $\lambda_{\vec{k}\nu}$ must be determined from the requirement that the Hamiltonian (6), after inserting into it Eq. (7), should take the standard form

$$H_P = \sum_{\vec{k}\nu} \hbar \omega_{\vec{k}\nu} \left(a^*_{\vec{k}\nu} a_{\vec{k}\nu} + \frac{1}{2} \right). \tag{8}$$

Making use of the well-known vectorial identities, equations of motion for the fields and their continuity properties at the boundaries, together with the orthogonality properties of the different solutions, it can be shown that this is achieved with

$$\lambda_{\vec{k}\nu} = \left(\frac{\hbar \omega_P^2}{8\pi A \omega_{\vec{k}\nu}} \right)^{1/2} \left[\int_{-a}^{a} \vec{P}^*_{\vec{k}\nu}(z) \vec{P}_{\vec{k}\nu}(z) \, \mathrm{d}z + \right.$$
$$\left. + \frac{\omega_P^2}{(4\pi c)^2} \int_{-\infty}^{\infty} \vec{A}^*_{\vec{k}\nu}(z) \vec{A}_{\vec{k}\nu}(z) \, \mathrm{d}z - \mathrm{i} \frac{\omega_P^2}{4\pi c \omega_{\vec{k}\nu}} \int_{-a}^{a} \vec{A}^*_{\vec{k}\nu}(z) \vec{P}_{\vec{k}\nu}(z) \, \mathrm{d}z \right]^{-1/2}. \tag{9}$$

We must still choose some normalization condition to fix the constants $C_{\vec{k}\nu}$. We choose

$$\int_{-a}^{a} \vec{P}^*_{\vec{k}\nu}(z) \vec{P}_{\vec{k}\nu'}(z) \, \mathrm{d}z = \delta_{\nu\nu'}, \tag{10}$$

thus obtaining

$$C_{\vec{k}\pm} = \frac{1}{\sqrt{a}} \left[\frac{\mathrm{sh}\, 2\alpha\, a}{2\alpha\, a} \left(1 + \frac{k^2}{\alpha^2} \right) \pm \left(\frac{k^2}{\alpha^2} - 1 \right) \right]^{-1/2}. \tag{11}$$

It is understood everywhere that the quantities $\omega_{\vec{k}\pm}$, ε, α and α_0 are functions of the wave vector $\vec{k}$ through the dispersion relations (1) and their definitions. The surface-polariton field is finally quantized by letting $a_{\vec{k}\nu}$ and $a^*_{\vec{k}\nu} \to a^+_{\vec{k}\nu}$ be annihilation and creation operators for surface polaritons, satisfying the usual boson commutation rules.

Although we performed the quantization of the surface-polariton field for a simple point-ion model of a dielectric slab, the result can be extended to a more general situation. To show this, we explicitly perform the integration indicated in Eq. (5) and then in Eq. (9). The result can be expressed in the following form:

$$\lambda_{\vec{k}\pm} = \left(\frac{\hbar\, \omega_{\vec{k}\pm}}{8\pi\, A} \right)^{1/2} |\varepsilon - 1| \left\{ \frac{\omega^2_{\vec{k}\pm}}{\omega_P^2} (\varepsilon - 1)^2 + \varepsilon\, a\, C^2_{\vec{k}\pm} \left[\frac{\mathrm{sh}\, 2\alpha\, a}{2\alpha\, a} \left(\frac{k^2}{\alpha^2} - \frac{k^2}{\alpha_0^2} \right) \pm \right. \right.$$

$$\left. \left. \pm \left(\frac{k^2}{\alpha^2} - 1 \right) \right] \right\}^{-1/2}. \tag{12}$$

Now, our point-ion model shows up explicitly only in the first term in the curly brackets, i. e. where ω_P appears. Thus, if we make the substitution

$$\frac{\omega^2}{\omega_P^2} (\varepsilon - 1)^2 \to \frac{\omega}{2} \frac{\mathrm{d}\varepsilon}{\mathrm{d}\omega}, \tag{13}$$

which evidently holds for this model, and regard ε on the right-hand side and at every other place as a general dielectric function, our formulae will describe surface polaritons in a solid slab with quite a general but real dielectric function[2 8]. If we neglect retardation, (i. e. if we let $c = \infty$ and therefore $\alpha = \alpha_0 = k$) all results in this section reduce to the quasi-static results obtained previously[3,4].

3. *The electron-surface-polariton interaction Hamiltonian and the electron energy-loss-function*

The Hamiltonian of a non-relativistic electron with mass m and charge e, moving in the surface-polariton field is:

$$\frac{1}{2m} (\vec{p} - \frac{e}{c} \vec{A}(r, t))^2 + e\, \Phi(\vec{r}, t), \tag{14}$$

where Φ and $\vec{A}$ are given by Eqs. (5) and (7), $\vec{r} = (\vec{\varrho}, z)$ and $\vec{p} = (p_{||}, p_z)$ are the electron position and momentum operators, respectively. Adding to this the free--surface-polariton Hamiltonian (8), we obtain the total Hamiltonian of the system in the form:

$$H = H_0 + H_{int},$$

$$H_0 = \frac{p^2}{2m} + H_p, \tag{15}$$

$$H_{int} = \sum_{\vec{k}\nu} [\Gamma_{\vec{k}\nu}(\vec{p}; \vec{\varrho}, z)\, a_{\vec{k}\nu} + \Gamma^{+}_{\vec{k}\nu}(\vec{p}; \vec{\varrho}, z)\, a^{+}_{\vec{k}\nu}].$$

The coupling functions $\Gamma_{\vec{k}\nu}$ are given by

$$\Gamma_{\vec{k}\nu}(\vec{p}; \vec{\varrho}, z) = e\, \lambda_{\vec{k}\nu} [\Phi_{\vec{k}\nu}(z) - \frac{\vec{p}}{m c} \vec{A}_{\vec{k}\nu}(z)]\, e^{i\vec{k}\vec{\varrho}} \tag{16}$$

and can be easily calculated with the help of Eqs. (5) and (12) for each surface-polariton mode. The term which contains combinations of two surface-polariton operators and which describes polariton-scattering processes will be neglected when considering only first-order processes.

We shall use the Fermi golden rule to find the probability for one-surface-polariton emission. The free-electron wave function is of the form

$$\psi_{\vec{\varkappa}}(\vec{r}) = \frac{1}{(2\pi A)^{1/2}} e^{i\vec{\varkappa}\vec{r}}, \tag{17}$$

where the parallel component of the electron momentum $\hbar\vec{\varkappa}_{||}$ is made discrete for convenience and the electron energy is $E = \hbar^2 \varkappa^2/2m$. Assuming the surface--polariton field initially in its ground state, we find the probability $P_{i\to f}$ of one--surface-polariton emission to be

$$P_{i\to f} = \frac{2\pi}{\hbar} |F_{\vec{k}\nu}(\vec{\varkappa}_i, \vec{\varkappa}_f)|^2\, \delta(E_i - E_f - \hbar\omega_{\vec{k}\nu}), \tag{18}$$

where

$$F_{\vec{k}\nu}(\vec{\varkappa}_i, \vec{\varkappa}_f) = \frac{1}{2\pi} \int_{-\infty}^{\infty} dz\, e^{-i\Delta\varkappa_z z}\, \Gamma^{*}_{\vec{k}\nu}(\hbar\vec{\varkappa}_i; 0, z). \tag{19}$$

$\hbar\vec{\varkappa}_i$ and $\hbar\vec{\varkappa}_f$ are the initial and final electron momenta, respectively, and

$$\Delta\varkappa_z = \varkappa_{zf} - \varkappa_{zi}, \qquad \vec{\varkappa}_{||i} = \vec{\varkappa}_{||f} + \vec{k}. \tag{20}$$

The total emission probability per electron P is obtained by summing Eq. (18) over all electron and polariton final states and by dividing it by the incoming electron

flux density. The conservation of the parallel momentum then eliminates the summation over $\vec{\varkappa}_{\|f}$, while the δ function in energy can be used to eliminate the integration over $\varkappa_{zf}$. Finally, we arrive at

$$P = \left(\frac{2\pi}{\hbar}\right)^2 \sum_{\vec{k}\nu} \frac{m^2}{\hbar^2 \varkappa_{zi} \varkappa_{zf}} |F_{\vec{k}\nu}(\vec{\varkappa}_i, \vec{\varkappa}_f)|^2, \tag{21}$$

where the final electron momentum $\varkappa_{zf}$ is now fixed:

$$\varkappa_{zf} = \left(\varkappa_{zi}^2 + 2\vec{\varkappa}_{\|i} \cdot \vec{k} - k^2 - \frac{2m\omega_{\vec{k}\nu}}{\hbar}\right)^{1/2}. \tag{22}$$

In contrast to classical treatments, Eq. (21) also includes corrections coming from the quantum nature of the electron and is, therefore, correct even for slow electrons. These corrections become unimportant whenever we can make the so-called fast-electron approximation

$$\Delta\varkappa_z \simeq \varkappa_{zi}\left(1 - \frac{\hbar\omega_{\vec{k}\nu}}{E_{zi}}\right)^{1/2} - \varkappa_{zi} \simeq -\frac{\omega_{\vec{k}\nu}}{v_{zi}}, \tag{23}$$

i. e. whenever $E_{zi} \gg \hbar\omega_{\vec{k}\nu}$. In this case, the electron represents just the classical current.

In transmission experiments, electrons with energies of several tens keV are used; it is, therefore, perfectly correct to use the approximation (23). Using also

$$\sum_{\vec{k}} = \frac{A}{(2\pi)^2}\int_0^{2\pi} \mathrm{d}\varphi \int k\,\mathrm{d}k = \frac{A}{(2\pi)^2}\int_0^{2\pi} \mathrm{d}\varphi \int k \left|\frac{\mathrm{d}k}{\mathrm{d}\omega}\right| \mathrm{d}\omega,$$

with the obvious meaning of the quantities, we can convert Eq. (21) into either the angular-distribution function for electrons $P(k)$ or the electron energy-loss function $P(\omega)$. We quote here the result for $P(\omega)$ and for normal electron incidence, which is the geometry used most often. Performing all the necessary integrations (from Eq. (4) to Eq. (5) and then from Eq. (16) to Eq. (19)) and using Eqs. (11), (12) and (13), one finds

$$P(\omega) = P_+(\omega) + P_-(\omega),$$

$$P_\pm(\omega) = 4\frac{e^2}{\hbar v^2}\frac{k}{a_0}\left|\frac{\mathrm{d}k}{\mathrm{d}\omega}\right| \omega \frac{(\varepsilon - 1)^2}{-\varepsilon}\frac{k^2}{\varphi_0^4 \varphi^4}$$

$$\left| \zeta^2 \begin{pmatrix} \sin \frac{\omega a}{v} \\ \cos \frac{\omega a}{v} \end{pmatrix} \pm a_0 \varepsilon \frac{\omega}{v} \left(\frac{v}{c}\right)^2 \begin{pmatrix} \cos \frac{\omega a}{v} \\ \sin \frac{\omega a}{v} \end{pmatrix} \right|^2$$

$$\times \frac{}{\left[\frac{\omega}{2} \frac{\mathrm{d}\varepsilon}{\mathrm{d}\omega} + \varepsilon\right] \left[1 + \frac{k^2}{a^2} \mp \frac{a}{a_0} \left(\frac{\omega}{c}\right)^2 \begin{pmatrix} (\mathrm{ch}\, a\, a)^{-2} \\ (\mathrm{sh}\, a\, a)^{-2} \end{pmatrix}\right] - \varepsilon \left(1 + \frac{k^2}{a_0^2}\right)} \tag{24}$$

where $k = k_{\pm}(\omega)$ and is just the inverse function of $\omega_{\pm}(k)$. In Eq. (24) we have introduced

$$\varphi_0^2 = a_0^2 + \left(\frac{\omega}{v}\right)^2, \qquad \varphi^2 = a^2 + \left(\frac{\omega}{v}\right)^2, \qquad \zeta^2 = k^2 + \left(\frac{\omega}{v}\right)^2 - \left(\frac{\omega}{c}\right)^2 (1 + \varepsilon). \tag{25}$$

The range of ω in Eq. (24) is, of course, determined by the solution of the dispersion relation (1) and is, therefore, different for different solids, i. e. for different ε.

Because of our approximations, Eq. (24) must correspond to the classical result obtained by Kröger[20] taken with a real dielectric function. Indeed, if in his result we use the limit

$$\lim_{\mathrm{Im}\, \varepsilon \to 0} \frac{1}{a_0 \varepsilon + a\, (\mathrm{th}\, a\, a)^{\pm 1}} = \frac{-i \pi \delta (k - k_{\pm}(\omega))}{\left| \frac{\partial}{\partial k} (a_0 \varepsilon + a\, (\mathrm{th}\, a\, a)^{\pm 1} \right|_{k = k(\omega)}}$$

and integrate over k, we immediately arrive at Eq. (24).

4. *Surface polaritons observed in electron-transmission spectroscopy*

As pointed out in the Introduction, the main difficulty in observing the polariton character of surface excitations lies in the low angular resolution of the experimental apparatus. In a classical transmission experiment, the analyzer collects all electrons scattered up to some finite angle from the direction of the incident beam. The analyzer cut-off wave vector $k_c \sim k_0 \Theta_c$ (k_0 is the incident-electron wave vector) is usually smaller than the polariton-decay cut-off wave vector ($\sim 10\ \mathrm{nm}^{-1}$) but is larger than the typical wave vector $k_p = \omega_P/c$, below which the retardation effects become important ($k_p \sim 10^{-2}\ \mathrm{nm}^{-1}$ for metals and $\sim 10^{-4}\ \mathrm{nm}^{-1}$ for dielectrics). Therefore, surface polaritons, i. e. retardation effects by electron-transmission spectroscopy can be seen only if a high-resolution (less than 10^{-5} rad) apparatus is used.

We describe the influence of the experimental apparatus in the following manner:

(i) We introduce, in the k space, the cut-off wave vector k_c which is directly related to the aperture of the spectrometer.

(ii) To describe the finite energy resolution of the apparatus, we folded the theoretical spectrum by an appropriate energy-response function. This is performed formally by replacing the δ function in energy (implied in our theoretical spectrum) by a more realistic function of the Gaussian or Lorentzian shape.

In analyzing surface energy losses of electrons in a dielectric slab and comparing their theoretical results with experiments on LiF[29], Chase and Kliewer[22] (*CK*) concluded that retardation corrections were negligible for small slab thicknesses. They pointed out that the coupling of the ω_+ polariton mode (which is influenced mostly by the retardation of the electromagnetic field) with electrons is very weak in comparison with the coupling of the ω_- mode, because of the different polarization properties. To illustrate this, we calculated Eqs. (21)—(24) numerically and compared our theory with *CK*'s dielectric theory[22] and with experiments[29]. We used the same parameters as *CK* did in their work. The dielectric function was of the form

$$\varepsilon(\omega) = \varepsilon_\infty \left[1 + \frac{\omega_p^2}{\omega_T^2 - \omega^2}\right],$$

where

$$\omega_P^2 = \left(\frac{\varepsilon_0}{\varepsilon_\infty} - 1\right) \omega_T^2.$$

Figure 1 shows the result of our calculation (full curve) plotted against *CK*'s Fig. 7[22] (broken curve). As can be seen, both calculations are consistent with experiments (dotted curve) and with each other. Of course, for thicker slabs, the contribution from bulk *LO* phonons, which is not included in our theory, should appear on the high-energy side of the spectrum in both the experiments and the dielectric theory.

In Fig. 2 we compare the separate contributions of the two surface polaritons (P_+, P_-) to the loss spectrum, with the experimental spectrum[29]. The contribution of the ω_+ surface polariton in a thin slab is completely different in shape and is an order of magnitude smaller than that of the ω_- mode, as a result of its weak coupling with the electron.

Such behaviour seems to confirm *CK*'s conclusion[22]. However, two things should be noted. First, the dispersion of surface polaritons in a dielectric slab starts from a finite value ω_T, so that only photons with frequencies higher than ω_T contribute to the mixed excitations. Second, for the angular resolution of $\Theta_c \sim$ $\sim 10^{-4}$ rad and the electron energy of 25 keV, we obtain a cut-off wave vector $k_c = 225\ k_p$ for the polariton. This means that the contribution of excitations from the „retarded" ($k \lesssim k_p$) region of surface-polariton dispersion relations is negligible compared with that for the „non-retarded" region ($k > k_p$). In other words, surface phonons dominate in the spectrum. With higher angular resolution, one should, in principle, observe retardation effects in the spectrum. We illustrate these two points for the case of a metallic slab.

The frequencies of the two surface modes in a metallic slab start from zero, so one should a priori except a more pronounced photon character of the polariton

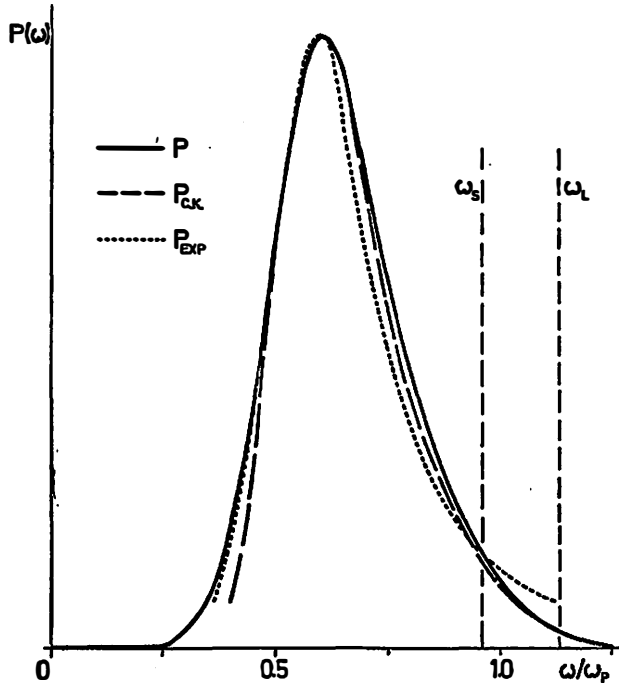

Fig. 1. The energy-loss spectrum $P(\omega)$ in relative units for 25-keV electrons normally transmitted through a 24 nm thick LiF foil ($\varepsilon_\infty = 1.90, \varepsilon_o = 8.81, \omega_T = 5.76 \times 10^{13}\ s^{-1}$). The energy resolution of the spectrometer is described by the Gaussian of a half-width of 0.01 eV and the angular resolution is determined by $\Theta_c \approx 10^{-4}$ rad.

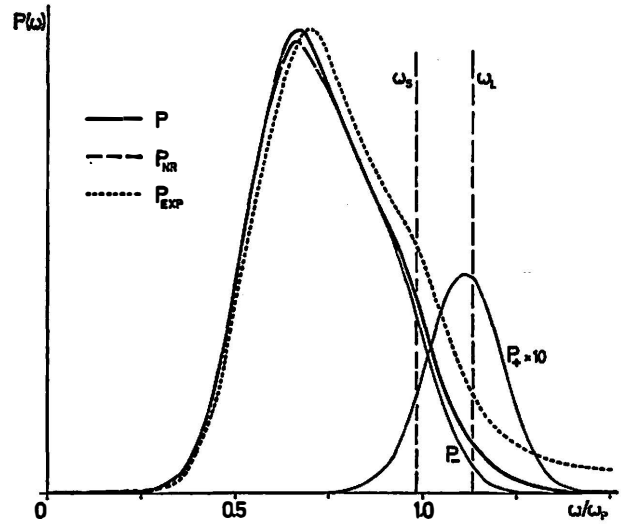

Fig. 2. The same data as for Fig. 1, but with a 70 nm thick Li foil. The retarded (full) and non-retarded (broken) curves are almost the same and are both in agreement with the experimental (dotted) curve.

and a stronger influence of the retardation on the electron energy-loss spectrum. The metal is described by the long-wavelength free-electron dielectric function

$$\varepsilon(\omega) = 1 - \frac{\omega_P^2}{\omega^2}, \tag{26}$$

where ω_P is the electronic plasma frequency. Inserting this dielectric function into Eq. (1), we obtain dispersion relations of surface polaritons in a metallic slab.

In Fig. 3a we compare the electron energy-loss spectrum given by the retarded (full curve) and non-retarded (dotted curve) theory for two different values of the cut-off wave vector k_c. As can be seen, the difference between the retarded and non-retarded curves is very small for $k_c = 4\,k_p\,(\Theta_c \simeq 2 \times 10^{-4})$ except in the very low energy region where the polariton character of surface excitations shows up. If we suppose that the angular resolution is an order of magnitude better, we can select electrons scattered by polaritons deep in the »retarded« region: $k_c = 0.7\,k_p$ means that we collect electrons scattered at an angle of up to approximately 4×10^{-5} rad. In this case, the retarded theory and the non-retarded theory give completely different results.

To make the analytical behaviour of the energy spectrum more apparent, let us use the approximate solution of the dispersion relation (1) for a metallic film in the region of small ($k < k_p$) wave vectors[30]

$$k_{\pm}^2 \sim \left(\frac{\omega}{c}\right)^2 \left[1 + \left(\frac{\omega}{\omega_P}\right)^2 (\mathrm{th}^2\, k_p\, a)^{\pm 1}\right]. \tag{27}$$

Inserting (27) into (24), we find for the low-energy region of the spectrum

$$P_{\pm}(\omega) \simeq 4\,\frac{e^2}{\hbar\, c}\,\frac{1}{\omega_P}\left(\frac{v}{c}\right)^2 (\mathrm{th}\, k_p\, a)^{\pm 1} \left[\frac{\omega}{\omega_P}\,\frac{v}{c}\,(\mathrm{th}\, k_p\, a)^{\pm 1} \begin{pmatrix} \cos\dfrac{\omega a}{v} \\ \sin\dfrac{\omega a}{v} \end{pmatrix} \mp \begin{pmatrix} \sin\dfrac{\omega a}{v} \\ \cos\dfrac{\omega a}{v} \end{pmatrix}\right]^2. \tag{28}$$

We see that $P_+(\omega) \sim (\omega/\omega_P)^2$, while $P_-(\omega) \sim$ const when ω approaches zero. With increasing thickness of the slab, both modes give equal contributions to the spectrum, showing oscillatory behaviour in energy. This is completely different from the result of the quasi-static theory, where the ω_+ mode always contributes to the high-energy side, $\omega_s < \omega < \omega_P$.

The same point can also be illustrated by examining the angular-distribution function $P(k)$ rather than $P(\omega)$ (Fig. 3b) (k is directly proportional to the scattering angle Θ for electrons). $P(k)$ is obtained from Eq. (24), if we put $\mathrm{d}k/\mathrm{d}\omega = 1$ and express every quantity as a function of k. As can be seen from Fig. 3b, at $k < k_p$, $P_+(k)$ is much smaller than $P_-(k)$: $P_+(k \to 0) \to 0$, $P_-(k \to 0) \sim$ const. At $k \gtrsim 3k_p$, the retarded (full) and non-retarded (broken) curves coincide.

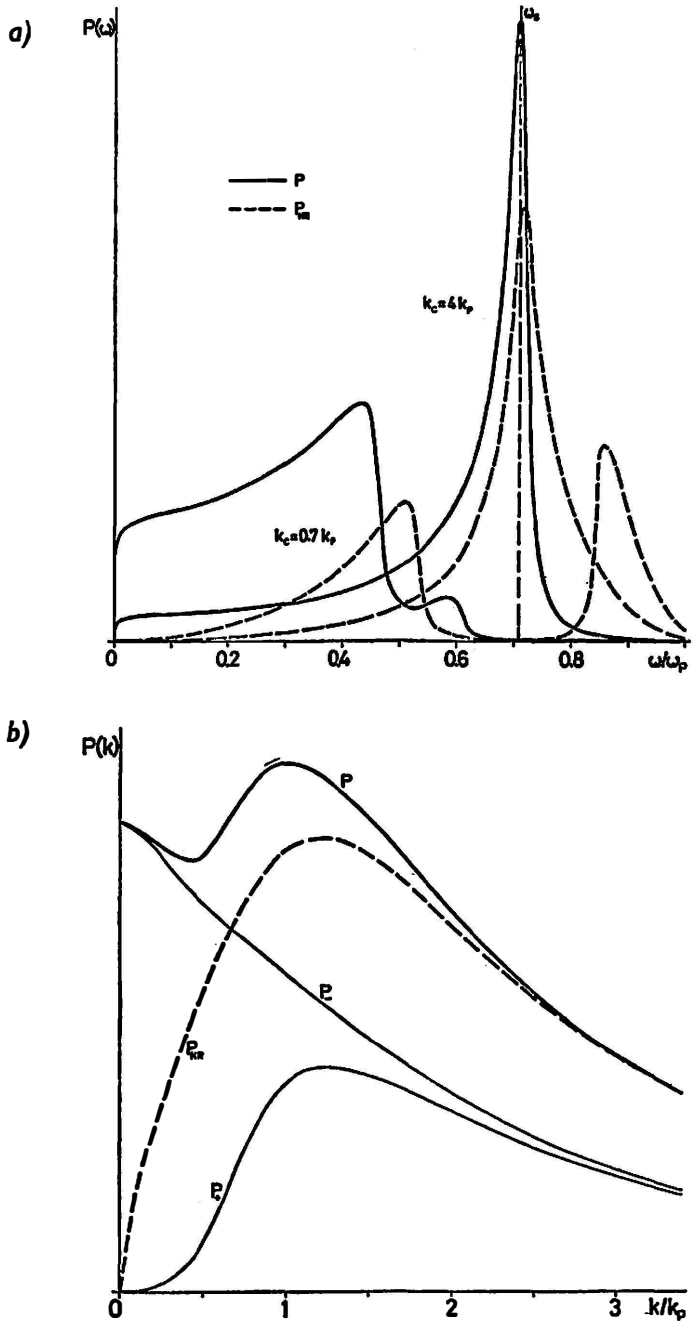

Fig. 3. The loss spectrum in relative units (*a*) $P(\omega)$ and (*b*) $P(k)$ for 75-keV electrons normally transmitted through a 16 bm thick Al foil ($\hbar\omega_p = 15.0$ eV). The Lorentzian with 0.15-eV half--width was used as the energy-response function (Fig. 3a).

It is also instructive to discuss the influence of retardation on the probability for ω_--mode emission. Taking the limit $c \to \infty$ in Eq. (24), we obtain the quasi-static result[3,4]

$$P_-^{NR}(\omega) = \frac{4}{a}\frac{e^2}{\hbar v^2}\frac{k_-^2}{\left[k_-^2 + \left(\frac{\omega}{v}\right)^2\right]^2}\frac{1-\varepsilon}{\varepsilon(\varepsilon+1)}\cos^2\frac{\omega a}{v}, \tag{29}$$

where

$$k_- = \frac{1}{2a}\ln\frac{\varepsilon - 1}{\varepsilon + 1}.$$

In the region $\omega \ll \omega_P$, which is under consideration, the ratio of Eq. (29) to Eq. (24) is

$$\frac{P_-^{NR}(\omega)}{P_-(\omega)} \simeq \left(\frac{\omega}{\omega_P}\right)^2 \frac{\operatorname{th} k_p a}{(k_p a)^3}, \tag{30}$$

so that the retarded theory always gives a greater probability for ω_--mode emission, especially for thicker films.

As is well known[30], retardation strongly influences the dispersion relation of the high-frequency ω_+ mode at $k \lesssim k_p$. Instead of approaching the frequency ω_P for $k \to 0$ monotonically, the ω_+ mode bends downwards and approaches the light line kc. For very thin films ($ak_p \ll 1$), the ω_+ mode takes a maximum $\omega = \omega_0$ at $k_0 \sim k_p$. It markedly enhances the density of states of surface excitations near ω_0 and therefore is responsible for the appearance of the high-energy maximum ($\omega_S < \omega_0 < \omega_P$), i. e. the splitting of surface loss peaks in the energy-loss spectrum. This behaviour is often screened by the more pronounced contributions of the ω_- mode (Fig. 2) and the bulk mode ($\omega = \omega_P$). Moreover, at $k \gg k_p$, the frequencies of both surface modes approach non-retarded values and tend towards the limiting surface-polariton frequency ω_S ($\varepsilon(\omega_S) = -1$). At this frequency, both modes give the same contribution to the spectrum (Fig. 3b). Therefore, the specific contribution of the ω_+ mode can apparently be detected only by a high-energy and high-angular-resolution spectrometer, as we have already pointed out.

For thicker films ($ak_p > 1$), the frequency of the ω_+ mode decreases and the ω_+ curve gradually approaches the ω_- curve. The contribution of the ω_+ mode to the spectrum moves downwards in energy and becomes comparable in magnitude with the contribution of the ω_- mode, but the separate contributions of the two surface modes cannot be easily distinguished.

Figure 4 shows the „theoretical" picture of the results of „high-angular-resolution" experiments[15,16] mentioned in the Introduction. We were not able to make a direct quantitative comparison with experimental data because the authors of Refs. 15 and 16 were concerned exclusively with the determination of surface-excitation dispersion relations in a thin Al film, so they presented only the experimental photographs of the electron energy-loss probability function. Figure 4

should, therefore, be compared with the intensity contour map obtained from photographic plates. We should emphasize that we have neglected polariton damping from the beginning, so that the intensity contour map we have obtained arises solely by the introduction of the energy-resolution function, thus taking into account the limiting sensitivity of the experimental set-up. In Fig. 4 we have chosen the same parameters as given in Fig. 1 by Petit et al.[16]. Comparison of Fig. 4 of this paper and Fig. 1 of Ref. 16 shows that the calculated and experimental results are in overall qualitative agreement. Furthermore, the highest intensities appear in the region where surface-polariton dispersion relations are close to the light line kc (the tail in the radiative region $\omega > kc$ is exclusively a consequence of the energy-response function introduced). It follows from the preceding discussion that this high-intensity region is produced mainly by the excitation of ω_- surface polaritons.

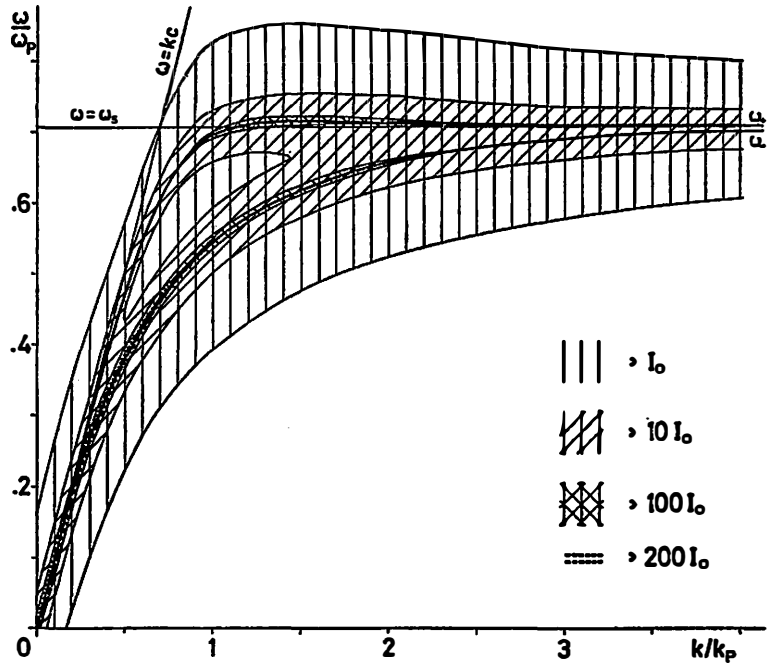

Fig. 4. The density profile $P(k, \omega)$ of the electron loss spectrum. Only the intensities larger than some (arbitrarily chosen) intensity I_0 are drawn. The density profile follows the retarded surface-plasmon dispersion curves $\omega_\pm(k)$. The data are the same as in Fig. 3.

Up to now we have discussed the single-excitation spectrum only, but multiple-excitation processes can also be taken into account. We notice that the ω_- mode gives a non-zero contribution to the electron spectrum at zero energy, as can be seen from Eq. (28) (in full contrast to the results of the quasi-static theory, see Eqs. (29) and (30)). Therefore, multiple emission of ω_- surface polaritons should strongly influence the low-energy part of the electron energy-loss spectrum.

Indeed, if we denote by E the electron energy loss due to all possible processes of surface-polariton excitations, we can write the full electron energy-loss spectrum $W(E)$ in the form[4,26]

$$W(E) = \frac{1}{2\pi} \int_{-\infty}^{\infty} dt\, e^{\frac{i}{\hbar} Et} \exp\left[\int d\omega\, P(\omega)\,(e^{-i\omega t} - 1)\right], \tag{31}$$

where $P(\omega)$ is the probability of single-polariton emission, Eq. (24). Generally, $W(E)$ consists of a δ line with some strength at $E = 0$ and a low-energy side-band. The strength of the δ line is determined by the probability that the electron excites none of surface polaritons (no-loss line) and is given by

$$\exp\left[-\int d\omega\, P(\omega)\right],$$

while the positive-energy side-band arises from the emission of all possible surface polaritons. It can be shown[31] that the behaviour of $W(E)$, Eq. (31), for low energy ($E \approx 0$) is governed by the behaviour of $P(\omega)$ for small ω ($\omega \simeq 0$). If $P(\omega)$ behaves as ω^{η} for $\omega \approx 0$, then the spectrum $W(E)$ depends on the magnitude of η. For $\eta > 0$, the strength of the no-loss line is finite and the positive-energy side-band starts from zero. For $0 \geq \eta > -1$, the strength of the no-loss line decreases, while the contribution from low-energy excitations becomes finite. At $\eta = -1$, the no-loss line disappears and the side-band has the integrable singularity, $W(E) \sim E^{-1+\varepsilon}$. The singularity in the spectrum becomes more pronounced with further decrease of η.

In our case, $P(\omega) \sim P_{-}(\omega) \sim$ const and $P_{+}(\omega) \sim \omega^2$ (Eq. (28)) for small ω, so that $\eta = 0$. Therefore, the strength of the no-loss line is reduced because of the excitations of ω_{-} surface polaritons, i. e. the shape of the spectrum of electrons for $E \cong 0$ is determined by their interaction with ω_{-} surface polaritons. Since we have shown that $P^{NR}(\omega) \sim \omega^2$ (Eq. (29)), this behaviour of the spectrum is not properly described in the quasi-static (non-retarded) theory.

5. *Sumary*

In this paper we have quantized the long-wavelength surface-polariton field in a thin film described by some real dielectric function $\varepsilon(\omega)$. This is a prerequisite for the theoretical investigations of the effects associated with surface polaritons in many physical situations.

We have applied the theory to the interaction of surface polaritons with electrons in electron-transmission experiments. The shape of the electron energy-loss spectrum has been calculated in the Born approximation and the corrections due to the retardation of the electromagnetic field have been discussed. We have shown that the retardation strongly influences the probabilities for single and also multiple excitation of surface modes in a metallic slab.

We have also confirmed the earlier conclusions that retardation corrections to the electron spectrum are more important for a metallic slab than for a dielectric one. However, in both cases, retardation effects cannot be resolved if the angular resolution of the experimental apparatus is not very high.

Note added in proof: After submitting this paper, we became aware of a recent article by W. Ekardt (Phys. Rev. B **23**, (1981) 3723). Like in our previous paper »Influence of Retardation on the Excitation of Surface Modes in Electron-Transmission Spectroscopy« (submitted to Phys. Rev. B in 1976, but not accepted for publication), Ekardt quantized the surface polariton field and calculated the electron-polariton retarded coupling constants. The results agree with ours. However, in this paper we pay more attention to the electron energy loss function rather than to the electron-surface polariton coupling constants and evaluate the transmitted high-energy electron spectra, compare them with experimental results, and discuss the retardation effects in the spectra.

References

1) K. L. Ngai, E. N. Economou and M. H. Cohen, Phys. Rev. Lett. **22** (1969) 1375;
2) K. L. Ngai, E. N. Economou and M. H. Cohen, Phys. Rev. Lett. **24** (1970) 61;
3) A. A. Lucas, E. Kartheuser and R. Badro, Phys. Rev. **B2** (1970) 2488;
4) M. Šunjić and A. A. Lucas, Phys. Rev. **B3** (1971) 719;
5) E. N. Economou and K. L. Ngai, Adv. Chem. Phys. **27** (1974) 265 and also K. L. Kliewer and R. Fuchs, ibid., 355;
6) See, for example, H. Raether, Excitations of Plasmons and Interband Transitions by Electrons, Springer Tracts in Modern Physics **88** (1980);
7) R. H. Ritchie, Phys. Rev. **106** (1975) 874;
8) M. Hattori and K. Yamada, J. Phys. Soc. Japan **18** (1963) 200;
9) T. Fujiwara and K. Ohtaka, J. Phys. Soc. Japan **24** (1966) 1326;
10) P. Schmüser, Z. Phys. **180** (1964) 105;
11) H. Boersch, J. Geiger, A. Imbusch and N. Niedrig, Phys. Lett. **22** (1966) 146;
12) J. B. Swan, A. Otto and H. Fellenzer, phys. stat. sol. **23** (1967) 171;
13) T. Kloos, Z. Phys. **208** (1968) 77;
14) A. Imbusch, Z. Phys. **216** (1968) 94;
15) R. Vincent and J. Silcox, Phys. Rev. Lett. **31** (1973) 1487;
16) R. B. Petit, J. Silcox and R. Vincent, Phys. Rev. **B11** (1975) 3116;
17) C. H. Chen, J. Silcox and R. Vincent, Phys. Rev. **B12** (1975) 64;
18) C. H. Chen and J. Silcox, Solid State Commun. **17** (1975) 273;
19) C. H. Chen and J. Silcox, Phys. Rev. Lett. **35** (1975) 390;
20) E. Kröger, Z. Phys. **216** (1968) 115;
21) A. A. Lucas and E. Kartheuser, Phys. Rev. **B1** (1970) 3588;
22) J. B. Chase and K. L. Kliewer, Phys. Rev. **B2** (1970) 4389;
23) J. Nkoma, R. Loudon and D. R. Tilley, J. Phys. C **7** (1974) 3547;
24) As was shown in Ref. 23, the damping of surface polaritons decreases for lower energies and momenta. In the low energy region, where retardation is most important, the damping can be neglected to rather a good approximation;
25) Almost the same argument as above applies here because the presence of the substrate affects mostly the high energy side of the surface-polariton dispersion relations; see Ref. 16;
26) M. S. Tomaš and M. Šunjić, Phys. Rev. **B12** (1975) 5363;
27) K. L. Kliewer and R. Fuchs, Phys. Rev. **144** (1966) 495;
28) Indeed, our results would then correspond to those which could be obtained from the general expression for the Hamiltonian density. (See L. D. Landau and E. M. Lifshitz, Electrodynamics of Continuous Media. Oxford: Pergamon 1960). By comparing the results of Ref. 26 with those of Ref. 23, one can easily check that these two procedures give the same answer;
29) H. Boersch, J. Geiger and W. Stickel, Phys. Rev. Lett. **17** (1966) 379;
30) E. N. Economou, Phys. Rev. **182** (1969) 539;
31) E. Müller-Hartmann, T. V. Ramahrishnan and G. Toulouse, Phys. Rev. **B3** (1973) 1102.

TEORIJA MEĐUDJELOVANJA ELEKTRONA S POVRŠINSKIM POLARITONIMA. PRIMJENA NA EKSPERIMENTE S PROLAZOM ELEKTRONA

M. S. TOMAŠ

Institut "Ruđer Bošković", Zagreb

Z. LENAC

Pedagoški fakultet, Rijeka

M. ŠUNJIĆ

Fizički odjel Prirodoslovno-matematičkog fakulteta, Zagreb

UDK 538.97

Originalni znanstveni rad

Formulirana je kvantno-mehanička teorija međudjelovanja nerelativističke nabijene čestice s površinskim polaritonima u kristalnom sloju te primijenjena na proračun vjerojatnosti emisije površinskih polaritona. Izračunata je, u Bornovoj aproksimaciji, funkcija raspodjele gubitaka energije elektrona relevantna u eksperimentima s prolazom elektrona. Diskutirani su utjecaji retardacije elektromagnetskog polja na energetski spektar elektrona pri prolazu kroz dielektrični i metalni sloj kod upada elektrona pod pravim kutem te za jednostruke i višestruke procese raspršenja.